

Starburst-driven superwinds in quasar host galaxies

Peter Barthel and Pece Podigachoski

Kapteyn Astronomical Institute, University of Groningen, The Netherlands.

pdb@astro.rug.nl

Belinda Wilkes

Harvard-Smithsonian Center for Astrophysics, Cambridge, Massachusetts, USA.

and

Martin Haas

*Astronomisches Institut, Ruhr Universität, Bochum, Germany.***ABSTRACT**

During five decades astronomers have been puzzled by the presence of strong absorption features including metal lines, observed in the optical and ultraviolet spectra of quasars, signalling in- and outflowing gas winds with relative velocities up to several thousands of km/sec. In particular the location of these winds – close to the quasar, further out in its host galaxy, or in its direct environment – and the possible impact on their surroundings have been issues of intense discussion and uncertainty. Using our Herschel Space Observatory¹ data, we report a tendency for this so-called associated metal absorption to occur along with prodigious star formation in the quasar host galaxy, indicating that the two phenomena are likely to be interrelated, that the gas winds likely occur on the kiloparsec scale and would then have a strong impact on the interstellar medium of the galaxy. This correlation moreover would imply that the unusually high cold dust luminosities in these quasars are connected with ongoing star formation. Given that we find no correlation with the AGN strength, the wind feedback which we establish in these radio-loud objects is most likely associated with their host star formation rather than with their black hole accretion.

Subject headings: galaxies: formation — galaxies: starburst — galaxies: high-redshift — infrared: galaxies — quasars: absorption lines

¹Herschel is an ESA space observatory with science instruments provided by European-led Principal Investigator consortia and with important participation from NASA

1. Introduction

Soon after the discovery of quasi-stellar radio sources, QSRs, in 1963, blue-shifted absorption features were found (Burbidge et al. 1966) in the optical (rest-frame ultraviolet) spectra of distant (high-redshift, $z > 1.5$) QSRs and of their radio-quiet counterparts, quasi-stellar objects (QSOs). The significantly lower redshift of most of these lines led to the conclusion that they originate in gas along the line-of-sight, opening an important new window to study the distribution and properties of intervening galaxies and gas clouds (Blades et al. 1988; Weymann et al. 1991). Decades of research have revealed the diversity of these absorbers (e.g., Bechtold 2002), including intervening primordial gas clouds, enriched haloes of intervening galaxies, and outflowing circumnuclear gas winds in the quasar host galaxy, among others. The identity of one class of absorption lines, associated, metal-rich, narrow absorption lines, remains elusive. These associated metal absorbers, seen mostly through ultraviolet C^{3+} (C IV) and Mg^+ (Mg II) absorption, are narrow and strong, have velocity widths less than ~ 300 km/sec and rest-frame equivalent widths, REWs, up to several Å, and occur (Foltz et al. 1986; Vestergaard 2003) within a velocity of a few thousand km/sec of the quasar. The class is defined by $|v| < 5000$ km/sec; both infall (negative $z_{em} - z_{abs}$) and outflow (positive $z_{em} - z_{abs}$) occur. Detailed study (e.g., Williams et al. 1975; Sargent et al. 1982; Hamann et al. 2001) of certain associated metal absorber systems, using fine-structure line information, has indicated that at least some are located at ~ 10 kpc of the central ionizing continuum source, however this is not confirmed for the class as a whole.

Quasar outflows are important as they remove gas from their host galaxy and thereby the fuel for the AGN accretion as well as the material for star formation. Estimates of the mass of the associated outflowing gas and its impact on the AGN host galaxy are a function of its distance and coverage factor, both of which are unknown. Nearby Mk 231 represents an intriguing case of this, so-called negative feedback. Its luminous far-infrared emission classifies this low-luminosity QSO as an Ultraluminous Infrared Galaxy, ULIRG, in which the far-IR emission implies a starburst galaxy nature (e.g., Surace et al. 1998). Integral field spectroscopy (Rupke & Veilleux 2013) has indicated the presence of massive associated absorbing winds, covering wide angles on the kpc-scale, suggesting sufficient outflowing material to have a significant impact on the galaxy. The ultimate driving mechanism for these winds could be the starburst, the AGN, or their combination. Mk 231 may represent the low luminosity equivalent of the Sloan Digital Sky Survey quasars for which a statistical effect was reported (Shen & Ménard 2012), attributing associated Mg II absorption to host galaxy star formation, the latter manifested by enhanced optical [O II] emission. In this Letter we report further evidence favoring that associated metal absorbers in quasars originate in starburst-driven winds.

2. Observations and results

Our group (Podigachoski et al. 2015; Podigachoski et al. 2016) has carried out far-infrared imaging/photometry of the complete sample of 62 $z > 1$ radio galaxies and QSRs in the 3C catalogue, using guaranteed time on the Herschel Space Observatory (Pilbratt et al. 2010), under projectcode GT1_pbarthel1, project title *The Herschel Legacy of distant radio-loud AGN*. Our spectral energy distribution (SED) modeling yields substantial cold dust luminosities for a significant subset of QSRs and radio galaxies, which we attribute to prodigious host galaxy star formation. Standard conversion formulae (Kennicutt 1998) yield star formation rates, SFRs, in the range of $\sim 150 - 900 M_{\odot}/\text{year}$ for one-third of the sample, and upper limits of $\sim 200 M_{\odot}/\text{year}$ for the other two-thirds of the sample: in fact, several of the 3C objects classify as (radio-loud) ULIRGs.

Considering those nine sample 3C QSRs for which high resolution optical (restframe ultraviolet) spectra are available in the literature, it is striking that the two strongest star-formers, 3C 298 (SFR=930 M_{\odot}/year) and 3C 205 (SFR=700 M_{\odot}/year), are known (Anderson et al. 1987) to possess strong associated C IV absorption. In addition, another high SFR sample source, QSR 3C 190 (SFR=470 M_{\odot}/year), had been reported (Stockton & Ridgway 2001) to possess strong associated metal absorption (Mg II – unfortunately no C IV data available) while having optical starburst signatures. These results motivated us to analyse our Herschel photometry of a representative set of twelve $2 \lesssim z < 3$ 4C quasars which we had added to the complete 3C sample with the aim of extending the redshift coverage of powerful radio-loud AGN to $z \sim 3$. Being more distant, their radio luminosities are comparable to those of the 3C objects, and their radio spectra and morphologies are also consistent with those of the 3C sample. The 4C-subsample Herschel photometry is published elsewhere (Podigachoski 2016). The SED analysis led to an even more striking result: only three of these sources are detected in the long wavelength Herschel bands, hence experience extreme star formation, and all three, 4C 09.17 ($z=2.111$, SFR=1330 M_{\odot}/year), 4C 24.61 ($z=2.330$, SFR=1960 M_{\odot}/year), and 4C 04.81 ($z=2.586$, SFR=1570 M_{\odot}/year) have (Barthel et al. 1990) strong associated C IV absorption. This suggests that the absorption is physically connected to the star formation. Dust component fitting of the near-IR – far-IR SEDs followed the techniques described in detail in Podigachoski et al. (2015): Hönig & Kishimoto (2010) warm dust tori reradiating the central AGN illumination were combined with hot (1300K) black bodies, and with cold grey bodies measuring the star formation luminosities. Figure 1, which can be found in the online material, presents the twelve SEDs and dust component fits. These fits permit extraction of the AGN as well as star formation strengths.

FIG 1: TWELVE 4C MIR-FIR SEDs

Adding the relevant 3C data from Podigachoski et al. (2015), Table 1 lists SED-inferred AGN strengths, SFRs and upper limits for all high-redshift 3C and 4C QSRs for which high quality optical spectra of the C IV region are available, with their associated C IV absorption strengths and velocity information. Figure 2 presents the SFRs as function of the absorption line REWs.

TABLE 1: 3C/4C QSR, with SFR, AGN, CIV REW, and relative velocity Delta-v

FIG 2: PLOT SFR vs. CIV REW

From Table-1 and Figure-2 it is seen that low-SFR 3C and 4C QSRs display no, weak, intermediate and strong associated C IV absorption. On the other hand, the most prodigiously star-forming QSRs uniformly display very strong absorption. We stress that there is not a one-to-one correspondence between SFR and absorption strength, as is for instance illustrated by 3C 191, the prototypical (Williams et al. 1975; Hamann et al. 2001) associated metal absorbing QSR with SFR upper limit (Podigachoski et al. 2015) of $300 M_{\odot}/\text{year}$. However, considering the SFR intervals < 400 , $400\text{--}1000$, and $> 1000 M_{\odot}/\text{year}$ (indicated with grey scales), the median C IV REW strengths are 0.9\AA , 1.9\AA , and 3.8\AA , with standard deviations 1.8\AA , 1.8\AA , and 2.6\AA , respectively. To further test the significance of the apparent trend, we applied a median test. Grouping the sources into high ($>700 M_{\odot}/\text{year}$) and low SFR, the probability of finding no high SFR sources with $\text{REW} < 1.6\text{\AA}$ (the sample median) is 0.023. While this is a marginal result which should be confirmed using a larger sample, it is consistent with the 3C 190 result (Stockton & Ridgway 2001) and with the statistical SDSS trend (Shen & Ménard 2012), thereby providing further evidence for a relation between associated metal absorbers and star formation.

The sightline towards the compact optical/ultraviolet continuum source is extremely narrow, so the chance of detecting absorption depends on the coverage of the continuum source by absorbing material and should be studied in a statistical sense. The data indicate that the coverage increases with increasing star formation rate. This means that more of the central continuum source is covered by absorbing material in the strongest star-formers, such as 4C 04.81, 4C 24.61, and 4C 09.17. At the same time, even in QSRs with a modest or small SFR, there is still a chance of intercepting absorbing gas clouds, while unobstructed sight lines ($\text{REW}=0$) also exist. We conclude that the associated metal absorption is likely to be directly related to the level of star formation in these QSRs.

3. Discussion

Recalling that the $\text{SFR}=10 M_{\odot}/\text{year}$ starburst in the nearby galaxy M 82 occurs (Fenech et al. 2008) within a 0.5 kpc region, that its starburst-driven superwinds (Heckman et al. 1990) extend over at least 1 kpc from its center, and recalling the similar figures (Rupke & Veilleux 2013) in starburst-QSO Mk 231, the starbursts producing hundreds to thousands of solar masses per year in the host galaxies of the 3C/4C QSRs likely occur on scales of 1 – 10 kpc. Such kiloparsec-scale distances from the central continuum source are consistent with the analyses (Williams et al. 1975; Hamann et al. 2001; Sargent et al. 1982) of some systems displaying fine-structure lines, as mentioned earlier. In fact, C IV absorbing gas around starburst galaxies can extend up to distances as large as 200 kpc (Borthakur et al. 2013).

The SFR-absorption trend for the radio-loud QSRs reported here suggests therefore that star-

burst driven superwinds on the 1 – 10 kpc scale are responsible for the associated metal absorption. Within that scenario, the (generally adopted) assumption that cold dust emission is associated with star formation is consistent. The winds potentially constitute important contributors to the chemical enrichment (Hamann & Ferland 1999) of the host galaxies and their environments. It is interesting to note that optical quasars displaying associated metal absorption tend to be reddened with respect to unabsorbed quasars, consistent with their inferred dusty hosts. Following up on the C IV study of Vestergaard (2003), the first to report systematic reddening, Vanden Berk et al. (2008) and Shen & Ménard (2012) measure $E(B - V) \sim 0.03$ in quasars with associated Mg II absorption. Vanden Berk et al. (2008) moreover found that the ionization of the associated absorbing gas cloud is dependent on the relative velocity $\beta = \Delta v/c$ of the cloud, in the sense that higher β systems have lower ionization.

Quantitative assessment (distance, mass, energetics) of the absorbing clouds is difficult, as detailed information on their properties (ionization, density, velocity structure, abundance) is lacking. Adopting steradian-scale coverage of the continuum source at distances $\gtrsim 1$ kpc, the absorbing gas must be in thin sheets, for all reasonable values of neutral hydrogen columns N_{H} . As Hamann et al. (2001) have shown for the case of 3C 191, using high resolution, high S/N Keck data, the absorber can have a multicomponent nature. These authors consider a blow-out leftover from a nuclear starburst as a possible origin for the associated metal absorber in 3C 191.

In the meantime, we have other ways to address the wind properties. For the highest SFR objects in our sample, those having $\text{SFR} \sim 1000 M_{\odot}/\text{year}$, Salpeter-type IMF starbursts lasting at least 10^7 yrs (being the lifetime of supernova producing stars) will yield (Woosley & Weaver 1986) $\sim 0.1\%$ which is $\sim 10^7$ core-collapse supernovae, with associated mass loss of $\sim 10^8 M_{\odot}$ and total energy injection of $\sim 10^{58}$ ergs (adopting wind velocities of a couple of thousand km/sec). Alternatively, applying the superwind model formulae (Heckman et al. 1990) predicting the outflow properties from the starburst’s infrared luminosity while adopting a burst duration of 10^7 yrs, yields very similar numbers: instantaneous energy loss of $\sim 10^{44}$ erg/sec, and integrated mass and energy loss $\sim 10^8 M_{\odot}$ and $\sim 10^{58}$ ergs, respectively. These numbers are broadly in line with the results obtained by Hamann et al. (2001) for 3C 191. We conclude that the feedback impact (per starburst; outflow as well as inflow) is substantial. As stated already, the detailed properties of the absorption systems and their impact require further high dispersion spectroscopic studies.

Supporting evidence for the star formation origin of the kpc-scale enriched gas in the host galaxies of these QSRs is provided by the infrared spectroscopy of Wilman et al. (2000). These authors discovered extended metal emission, in the form of [O III], in the dusty Ly- α nebulae of several of the objects of the present study. It is furthermore interesting to note that sample QSR 4C 24.61, with its extreme star formation rate, is the QSR displaying the highest (Kronberg & Perry 1982) residual rotation measure, RRM, at radio wavelengths. This supports the suggestion (Watson & Perry 1991) that associated metal absorbers are connected to the starburst-ionized ISM which is responsible for the Faraday rotation of the radio emission.

An issue of great importance concerns the nature of AGN feedback (e.g., Fabian 2012). Given that the radio luminosities of the QSRs under consideration, as well as their ultraviolet luminosities, are comparable while their wind properties differ, we suspect that the wind strengths are not driven by the AGN. However, dust extinction is at play and radio luminosity reflects AGN strength convolved with radio source environment (e.g., Barthel & Arnaud 1996). Integrated torus luminosities therefore represent a more reliable measure of the AGN (accretion) strength. Taking data from Table 1, we show in Fig. 3 the 3C/4C AGN strength as a function of the CIV equivalent widths: no correlation is seen. This strengthens our belief that – at least for these radio-loud objects – the wind feedback is not governed by the AGN, but by the contemporaneous star formation.

FIG 3: PLOT AGN vs. CIV strength

Finally, we are likely witnessing the extreme forms of processes which also occur in the low redshift universe. Given the starburst nature (Canalizo & Stockton 2000; Westhues et al. 2016) of the $z = 0.367$ FIR-ultraluminous QSR 3C 48 and the $z = 0.372$ FIR-luminous QSR 3C 351, respectively, their associated C IV absorption (Gupta et al. 2005; Mathur et al. 1994) is consistent with the same scenario. The earlier suggestions (Heckman et al. 1990) concerning the starburst driven superwind nature of metal absorption lines in FIR-bright quasars are consistent with our Herschel observations.

4. Conclusions

The occurrence of associated metal absorption, i.e., massive in- and outflowing winds, in radio-loud quasars is seen to increase with increasing star formation rate in the quasar host galaxies. This supports the view that these phenomena are physically related, is consistent with the picture that long-wavelength FIR emission is connected to star formation, and suggests that the wind feedback is driven by the star formation and not by the AGN.

PB acknowledges useful discussions with Fred Hamann, Michael Strauss, and Sylvain Veilleux. A constructive referee report with valuable suggestions is also gratefully acknowledged. The Herschel spacecraft was designed, built, tested, and launched under a contract to ESA managed by the Herschel/Planck Project team by an industrial consortium under the overall responsibility of the prime contractor Thales Alenia Space (Cannes), and including Astrium (Friedrichshafen) responsible for the payload module and for system testing at spacecraft level, Thales Alenia Space (Turin) responsible for the service module, and Astrium (Toulouse) responsible for the telescope, with in excess of a hundred subcontractors. HCSS/HSpot/HIPE is a joint development by the Herschel Science Ground Segment Consortium, consisting of ESA, the NASA Herschel Science Center, and the HIFI, PACS and SPIRE consortia.

REFERENCES

- Anderson, S. F., Weymann, R. J., Foltz, C. B., Chaffee, Jr, F. H. 1987, *AJ*, 94, 278
- Barthel, P. D., & Arnaud, K. A. 1996, *MNRAS*, 283, L45
- Barthel, P. D., Tytler, D. R., Thomson, D. 1990, *A&AS*, 82, 339
- Bechtold, J. 2002, in "Galaxies at high redshift", eds. I. Pérez-Fournon, M. Balcells, F. Moreno-Insertis, and F. Sánchez (Cambridge University Press), p. 131
- Blades, J. C., Turnshek, D. A., Norman, C. A. (eds.), 1988, "QSO Absorption Lines: Probing the Universe", *STScI Symposium Series Vol.2* (Cambridge University Press)
- Borthakur, S., Heckman, T., Strickland, D., Wild, V., Schiminovich, D. 2013, *ApJ*, 768, 18
- Burbidge, E. M., Lynds, C. R., Burbidge, G. R. 1966, *ApJ*, 144, 447
- Canalizo, G., & Stockton, A. 2000, *ApJ*, 528, 201
- Fabian, A. C. 2012, *ARA&A*, 50, 455
- Fenech, D. M., Muxlow, T. W. B., Pedlar, A., Beswick, R., Argo, M. K. 2008, *MNRAS*, 391, 1384
- Gupta, N., Srianand, R., Saikia, D. J. 2005, *MNRAS*, 361, 451
- Foltz, C. B., Weymann, R. J., Peterson, B. M., et al. 1986, *ApJ*, 307, 504
- Hamann, F. W., Barlow, T. A., Chaffee, F. C., Foltz, C. B., Weymann, R. J. 2001, *ApJ*, 550, 142
- Hamann, F., & Ferland, G. 1999, *ARA&A*, 37, 487
- Heckman, T. M., Armus, L., Miley, G. K. 1990, *ApJ*, 74, 833
- Hönig, S. F., & Kishimoto, M. 2010, *A&A*, 523, A27
- Kennicutt Jr, R. C. 1998, *ARA&A*, 36, 189
- Kronberg, P. P., & Perry, J. J. 1982, *ApJ*, 263, 518
- Mathur, S., Wilkes, B., Elvis, M., Fiore, F. 1994, *ApJ*, 434, 493
- Pilbratt, G. L., Riedinger, J. R., Passvogel, T., et al. 2010, *A&A*, 518, L1
- Podigachoski, P., Barthel, P. D., Haas, M., et al. 2015, *A&A*, 575, A80
- Podigachoski, P. 2016, "Star formation and AGN activity in distant massive galaxies", PhD Thesis, Univ. of Groningen

- Podigachoski, P., Rocca-Volmerange, B., Barthel, P., Drouart, G., Fioc, M. 2016, MNRAS, 462, 4183
- Rupke, D. S. N., & Veilleux, S. 2013, ApJ, 729, L27
- Sargent, W. L. W., Young, P., Boksenberg, A. 1982, ApJ, 252, 54
- Shen, Y. & Ménard, B. 2012, ApJ, 748, 131
- Stockton, A., & Ridgway, S. E. 2001, ApJ, 554, 1012
- Surace, J. A., Sanders, D. B., Vacca, W. D., Veilleux, S., Mazzarella, J. M. 1998, ApJ, 492, 116
- Vanden Berk, D., Khare, P., York, D. G., et al. 2008, ApJ, 679, 239
- Vestergaard, M. 2003, ApJ, 599, 116
- Watson, A. M., & Perry, J. J. 1991, MNRAS, 248, 58
- Weymann, R. J., Carswell, R. F., Smith, M. G. 1991, ARA&A, 19, 41
- Westhues, C., Haas, M., Barthel, P., et al. 2016, AJ, 151, 120
- Williams, R. E., Strittmatter, P. A., Carswell, R. F., Craine, E. R. 1975, ApJ, 202, 296
- Wilman, R. J., Johnstone, R. M., Crawford, C. S. 2000, MNRAS, 317, 9
- Woosley, S. E., & Weaver, T. A. 1986, ARA&A, 24, 205

Table 1. Associated CIV absorption line properties, AGN strength, and SFRs for 9 3C and 12 4C QSRs. The 3C AGN and SFR data were taken from Podigachoski et al. (2015); the 4C data result from the present analysis. The subsequent columns are: (1) 3C and 4C name; (2) IAU name (B1950); (3) redshift; (4) CIV rest-frame equivalent width, in Å (from Anderson et al. (1987) and Barthel et al. (1990); in some cases these are multiple systems, and asterisks mark values which may be slightly higher as the emission line profile cannot be measured precisely); (5) absorption system velocity w.r.t. systemic, in km/sec (positive for infall); (6) warm dust luminosity inferred AGN strength, in $10^{12} L_{\odot}/\text{yr}$; (7) cold dust luminosity inferred star formation rate and 3σ upper limits, in M_{\odot}/year

Name	IAU name	redshift	CIV REW (Å)	Δv (km/sec)	AGN strength ($10^{12} L_{\odot}/\text{yr}$)	SFR (M_{\odot}/yr)
3C 9	Q0017+154	2.014	0	0	17.1	< 310
3C 181	Q0725+147	1.388	0.9	~0	5.2	< 150
3C 191	Q0802+103	1.954	6.1	-610	17.0	< 300
3C 205	Q0835+580	1.533	3.2	590	27.9	700
3C 268.4	Q1206+439	1.400	1.9*	-1500	16.2	< 140
3C 270.1	Q1218+339	1.519	6.2*	-2260	12.7	390
3C 298	Q1416+067	1.440	4.5	120	29.2	930
3C 432	Q2120+168	1.805	0.3	-540	9.3	420
3C 454	Q2249+185	1.758	0.5	1420	10.5	620
4C -02.04	Q0038-019	1.672	0	0	21	< 240
4C 17.09	Q0109+176	2.155	5.4	190	8.1	< 490
4C -01.11	Q0225-014	2.038	0	0	7.7	< 250
4C 09.17	Q0445+097	2.111	6.7	~0	26	1330
4C 05.34	Q0805+046	2.876	0.6	~0	24	< 750
4C 28.40	Q1606+289	1.981	7.0	-910	9.5	< 370
4C 29.50	Q1702+298	1.927	0	0	4.1	< 250
4C 47.48	Q1816+475	2.223	0	0	15	< 150
4C 05.81	Q2150+053	1.978	0.8	1210	14	< 270
4C 05.84	Q2222+051	2.323	1.6	-990	31	< 540
4C 24.61	Q2251+244	2.330	3.8*	270	33	1960
4C 04.81	Q2338+042	2.586	2.4	330	37	1570

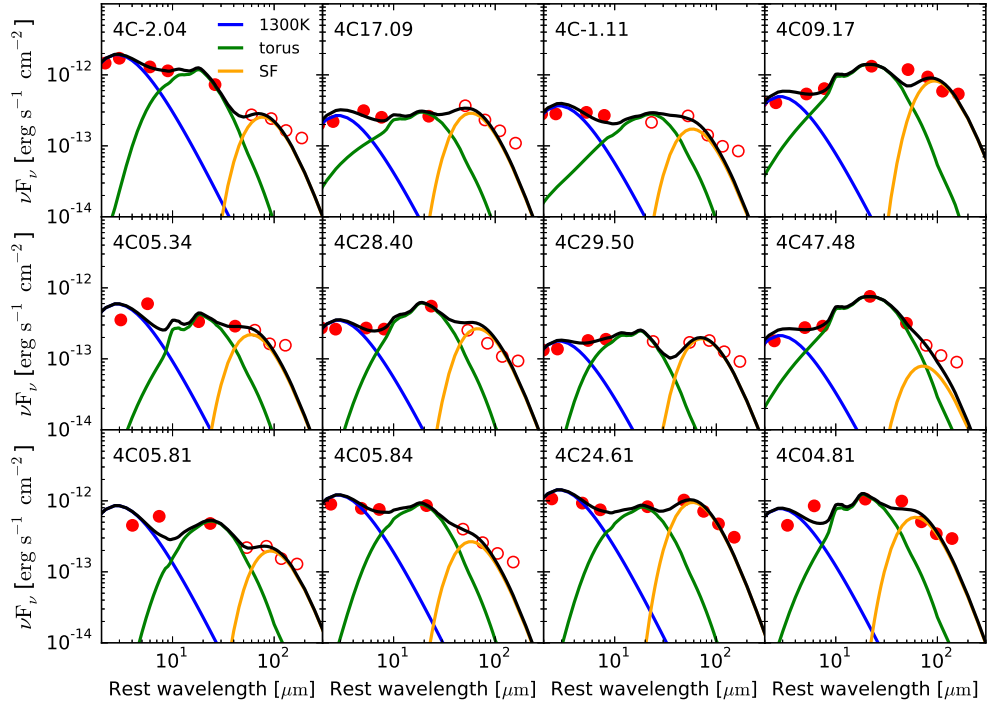


Fig. 1.— (Online material) NIR-MIR-FIR Spectral energy distributions for twelve Herschel detected 4C QSRs, with dust component fits. Open circles represent 3σ upper limits. The (green) warm torus models come from the library of Hönig & Kishimoto (2010), and yield the AGN strengths. The (yellow) modified blackbodies fitted to the long wavelength bands have fixed dust emissivity index $\beta = 1.6$ (chosen on the basis of our 3C analysis); their luminosities were subsequently converted to SFRs (see the text). As discussed in detail in Podigachoski et al. (2015), QSRs generally show hot, 1300K dust (blue curves). The black lines represent the sum of the three components.

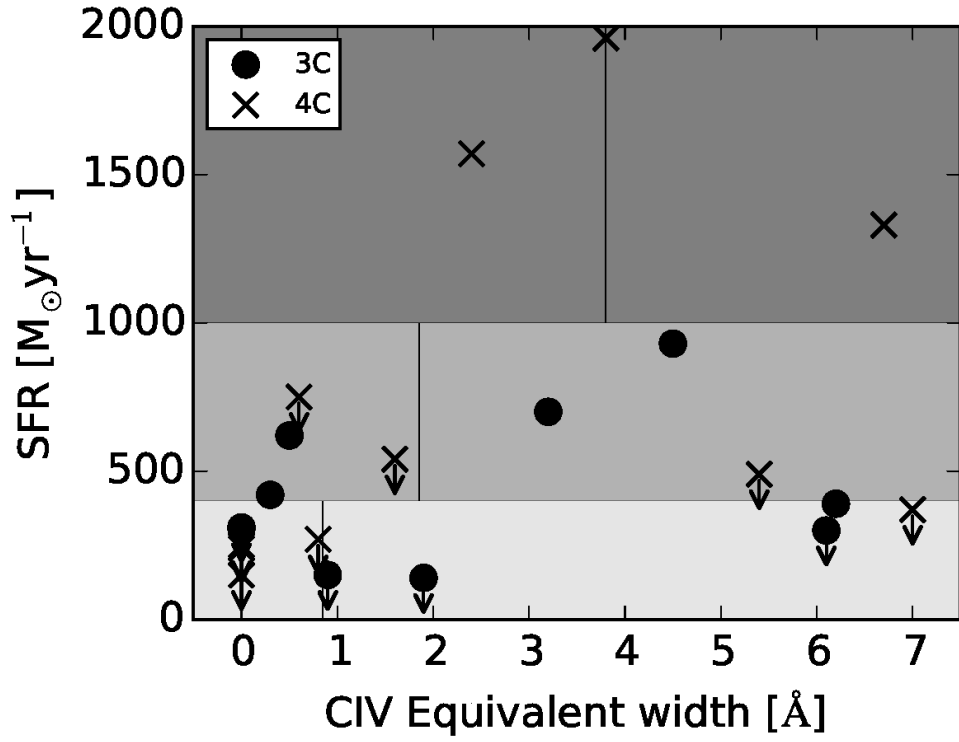


Fig. 2.— SFR vs. associated C IV absorption line strengths for 9 3C and 12 4C QSRs. The vertical lines indicate the median REW in the three separate SFR bins, marked with grey scales. These medians were obtained assuming all SFR upper limits to lie in the low SFR bin.

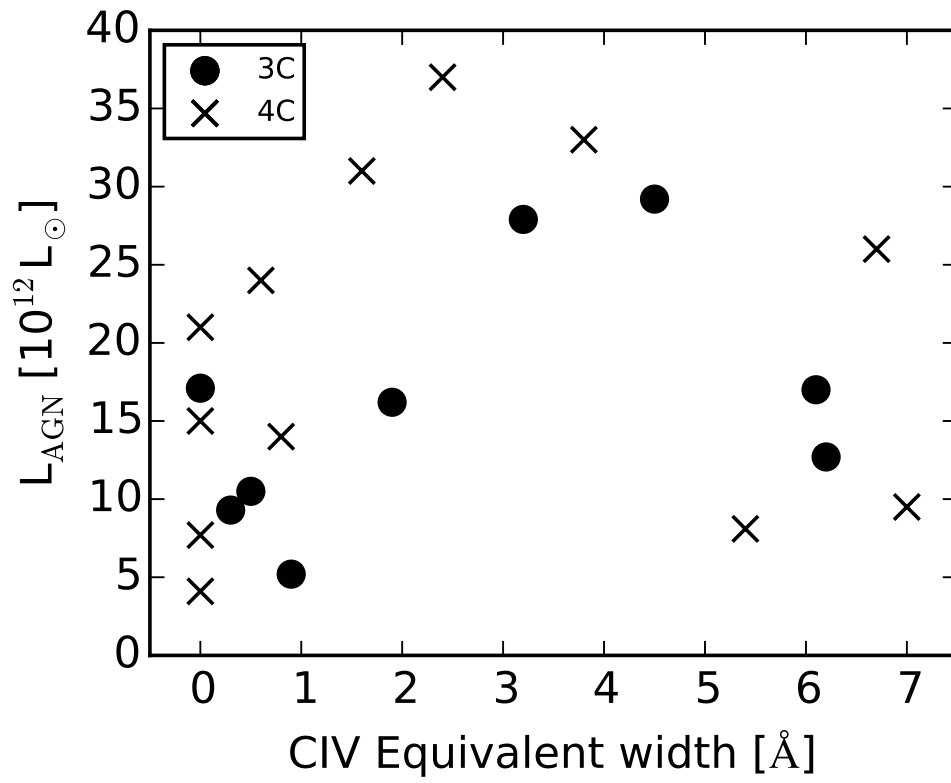


Fig. 3.— AGN strength vs. associated C IV absorption line strengths for 9 3C and 12 4C QSRs.